J|A|C|S COMMUNICATIONS

Published on Web 08/25/2009

Heavier Group 2 Metals and Intermolecular Hydroamination: A Computational and Synthetic Assessment

Anthony G. M. Barrett,*,‡ Christine Brinkmann,‡ Mark R. Crimmin,‡ Michael S. Hill,*,† Patricia Hunt,*,‡ and Panayiotis A. Procopiou§

Department of Chemistry, University of Bath, Claverton Down, Bath BA2 7AY, U.K., Department of Chemistry, Imperial College London, Exhibition Road, South Kensington, London SW7 2AZ, U.K., and GlaxoSmithKline Medicines Research Centre, Gunnels Wood Road, Stevenage, Hertfordshire SG1 2NY, U.K.

Received July 20, 2009; E-mail: msh27@bath.ac.uk

We have recently demonstrated that catalytic intramolecular hydroamination of aminoalkenes may be achieved through use of the d^0 metals of group 2 (Scheme 1).[1] In common with other metal-mediated transformations, the effect of ionic radius on reaction kinetics in organolanthanide(III) hydroamination catalysis is well-documented, and the reaction tends to proceed at lower rates with decreasing metal ionic radius.[2] This effect has been ascribed to the greater degree of coordinative saturation at the electrophilic metal center, increasing the energy of the transition state of the rate-determining alkene insertion step. In contrast to the relatively small change in the ionic radius of M^{3+} in going from lanthanum to lutetium (19.9%), descent in group 2 from magnesium to barium provides a drastically large change in M^{2+} ionic radius (87.5%).[3] Although detailed mechanistic studies have shown that the calcium complex **1** is a superior catalyst to the magnesium analogue **2** for the reaction depicted in Scheme 1, further empirical studies in our group and that of Roesky imply that this trend does not extend neatly to strontium and barium.[4,5] Rather, it appears likely that large variations in cation size and resultant charge density produce dramatic effects on reactivity across the series of M^{2+} cations.

To inform our understanding of the observations outlined above, we undertook a density functional theory (DFT) computational study with an initial aim of highlighting the intrinsic reaction barriers accommodated within the catalytic mechanism and the differing energetics implied by the relative effectiveness of the calcium and magnesium species **1** and **2**. In the interest of computational expense, these initial calculations were performed on a simple model system in which the aminoalkene was replaced by ammonia and ethene. Therefore, the process described explicitly relates to an intermolecular process rather than the intramolecular one described in our previous synthetic studies. The ancillary β-diketiminato ligands of **1** and **2** were also simplified by replacing the two *N*-aryl substituents with H atoms, and the analysis was extended to the heaviest members of group 2. In common with the previously reported lanthanide-based species, catalyst activation is rapid and necessarily exothermic and is unlikely to affect the rate of the reaction. Consequently, catalyst formation by initial protonolysis of an amido or alkyl precatalytic species was not computationally examined.

The catalytic cycle was broken down into component steps and associated structures (a full description of the steps included in the analysis is provided in the Supporting Information). Our results support rate-determining alkene insertion within a catalytic cycle dominated by Coulomb interactions, and the facility of the process is dependent upon the identity of the metal (Figure 1). In agreement with our experimental observations of intramolecular alkene hydroamination, the Ca-based cycle provided activation barriers ($\Delta G^{\ddagger}$) for alkene

Scheme 1

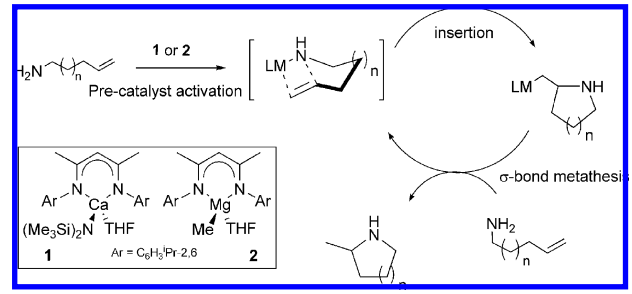

insertion (16.7 kcal mol^{-1}) and protonolysis of the aminoalkane intermediate (8.6 kcal mol^{-1}) that were significantly lower than the values of $\Delta G^{\ddagger}$ calculated for M = Mg (alkene insertion, 21.0 kcal mol^{-1}; protonolysis, 19.8 kcal mol^{-1}).

Alkene insertion into the M−N bond occurs via a four-center transition state that is highly polarized. During the insertion process, electron density equivalent to almost an entire electron is polarized onto the carbon atom adjacent to M (C^1) and is stabilized by the positive charge of the metal (Figure 2). As the electron density at C^1 increases, the nitrogen-based lobe is simultaneously depleted, and electron density is redirected into the newly forming C−N bond. Stabilization of the transition state may therefore be achieved by depletion of the negative charge at C^1 directly adjacent to the highly electropositive metal center, while the necessary accumulation of positive charge at C^2 would have a destabilizing effect. A metal that can be polarized toward C^2 and N and away from C^1 would also provide a stabilizing influence upon the transition state. The reduced barrier height for alkene insertion into a Ca−N versus a Mg−N bond

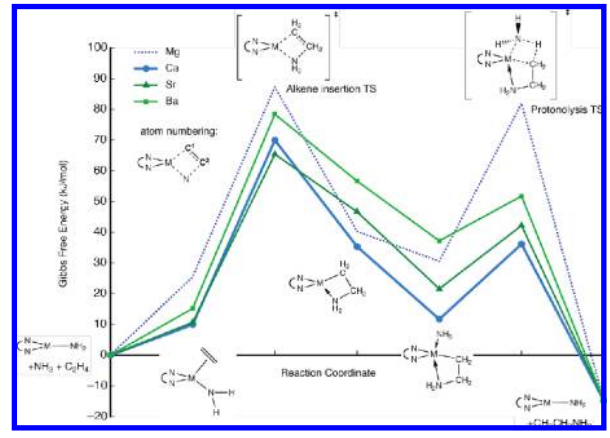

Figure 1. Free-energy profiles for hydroamination catalyzed by group 2 metals.

† University of Bath.
‡ Imperial College London.
§ GlaxoSmithKline Medicines Research Centre.

10.1021/ja905615a CCC: $40.75

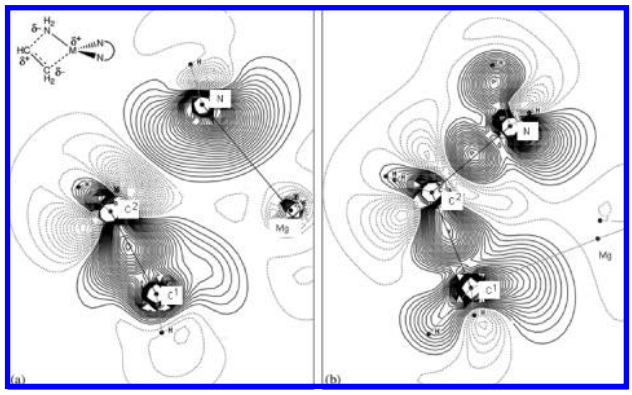

Figure 2. Electron density difference maps for the alkene insertion (a) transition state and (b) intermediate for the Mg-mediated cycle. The density difference is relative to a promolecule composed of spherical atoms; solid lines indicate areas of buildup in electron density, and dotted lines indicate areas of depletion. The slice shown was taken in the $C^1-C^2-N^3$ plane, and the contour interval is 0.003.

may therefore be viewed as the result of not only the greater polarity (and consequent superior ability to induce a dipole in the nonpolarized ethene substrate) of the Ca−N bond but also the greater polarizability of the Ca^{2+} cation.

This deduction was reinforced by analogous calculations with M as either Sr or Ba. Although both computed cycles also indicated rate-determining alkene insertion (Figure 1), the trend toward reduced barrier heights with increasing atomic weight did not continue. Although $\Delta G^{\ddagger}$ for insertion when M = Sr (15.5 kcal mol^{-1}) was slightly less than that when M = Ca, a significant increase was observed for M = Ba ($\Delta G^{\ddagger}$ = 18.6 kcal mol^{-1}). Following our postulate above, we attribute this latter result to the highly diffuse and thus weakly polarizing nature of the Ba atom, which is unable to sufficiently polarize the Ba−N bond or stabilize the charge accruing on C1 of the ethene C=C unit.

Although synthetic accounts of the more challenging intermolecular variant of this reactivity by organolanthanide catalysis are limited, vinyl arene hydroamination has been reported to proceed with good isolated yields and excellent anti-Markovnikov regioselectivity.[2,6] We thus carried out a preliminary study of intermolecular hydroamination catalysis of vinyl arenes and conjugated dienes with a variety of primary, secondary and N-heterocyclic amines. In line with the expectation provided by the DFT studies, stabilization of the incipient benzylic charge induced by formation of the proposed four-membered transition state provided exclusive access to the anti-Markovnikov products. The reactions were successfully carried out employing the homoleptic calcium and strontium amides $[M\{N(SiMe_3)_2\}_2]_2$ [M = Ca (**3**), Sr (**4**)], and typical results are summarized in Table 1. Analogous reactions with Mg- and Ba-based species were found to be very slow and are thus not included in further discussion.

In every case, strontium catalyst **4** was found to display a higher activity than the calcium complex **3**, and in general, comparable conversions were achieved in approximately half the reaction time. When less-active substrates were applied, the difference was even more significant (Table 1, entries 1−3).

Further insight into the improved catalytic performance of the strontium amide was provided by a kinetic analysis of the reaction of the cyclic secondary amine piperidine with styrene, employing an excess of styrene to provide a pseudo-first-order reaction. Although the exact rate law was not determined and substrate inhibition may play a key role,[1b] the addition of piperidine to styrene catalyzed by **3** and **4** provided two series of pseudo-first-order rate constants obtained

Table 1. Comparison of Calcium- and Strontium-Mediated Intermolecular Hydroamination

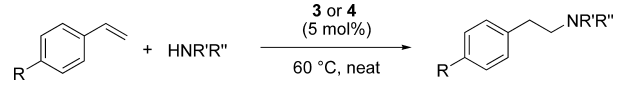

			3		4	
entry	R	amine	time (h)	conv (%)	time (h)	conv (%)
1	OMe	$PhCH_2NH_2$	168	17	144	63
2	Me	$PhCH_2NH_2$	60	70	28	84
3	H	$PhCH_2NH_2$	48	92	24	78
4	Cl	$NH(CH_2)_5$	24	60	17	79
5	Cl	$NH(CH_2)_4$	2	95	1	65

from ^1H NMR monitoring at four different reaction temperatures. Arrhenius analyses derived from the two sets of kinetic data afforded activation energies (E_a) of 12.7 and 17.2 kcal mol^{-1} for the calcium- and strontium-catalyzed reactions, respectively. Although the increased rate of hydroamination provided by the strontium amide **4** thus appears counterintuitive, Eyring analyses of the kinetic data provided a telling insight into the nature of the catalytic reactions. The values derived for the activation enthalpies ($\Delta H^{\ddagger}$ = 12.2 kcal mol^{-1} for **3** and 17.0 kcal mol^{-1} for **4**) were comparable to the E_a values. The entropy of activation ($\Delta S^{\ddagger}$) for **3** (−40.1 cal mol^{-1} K^{-1}), however, was found to be considerably more negative than that for **4** (−22.0 cal mol^{-1} K^{-1}), and thus, $\Delta G^{\ddagger}$ values of 24.1 and 23.4 kcal mol^{-1} were obtained for the reactions catalyzed by **3** and **4**, respectively, at 298 K. Use of the larger alkaline-earth cation (six-coordinate radii: Ca^{2+}, 114 pm; Sr^{2+}, 132 pm)[3] thus provides a distinct and influential entropic advantage that is most likely a reflection of the relative "tightness" of the four-membered insertion transition states required to assemble the substrate components about the respective group 2 metal centers. Although exactly analogous data have not been reported for any lanthanocene-catalyzed system, it is noteworthy that reported $\Delta S^{\ddagger}$ values for both inter- and intramolecular processes are on the order of −26.3 cal mol^{-1} K^{-1}, and it has been argued that the transition states are thus highly organized/constrained.[2,6] In conjunction with the influence of cation polarizability inferred from our gas-phase computational study, therefore, it is apparent that the hydroamination activity of the group 2 elements should not be viewed as simply "lanthanide-mimetic". Rather, their larger variations in size, electropositive character, and charge density may afford even greater scope for tuning and selection of complementary reactivity within a specific catalytic mechanism.

Supporting Information Available: Full experimental details for the DFT calculations, catalytic reactions, and kinetic analyses. This material is available free of charge via the Internet at http://pubs.acs.org.

Acknowledgment. We thank GlaxoSmithKline for the generous endowment (to A.G.M.B.), the Royal Society for a University Research Fellowship (to M.S.H.), and GlaxoSmithKline for generous support of our studies.

References

(1) (a) Crimmin, M. R.; Casely, I. J.; Hill, M. S. *J. Am. Chem. Soc.* **2005**, *127*, 2042. (b) Crimmin, M. R.; Arrowsmith, M.; Barrett, A. G. M.; Casely, I. J.; Hill, M. S.; Procopiou, P. A. *J. Am. Chem. Soc.* **2009**, *131*, 9670.
(2) Hong, S.; Marks, T. J. *Acc. Chem. Res.* **2004**, *37*, 673.
(3) Shannon, R. D. *Acta Crystallogr.* **1976**, *A32*, 751.
(4) (a) Barrett, A. G. M.; Crimmin, M. R.; Hill, M. S.; Kociok-Köhn, G.; Procopiou, P. A. *Inorg. Chem.* **2008**, *47*, 7366. (b) Arrowsmith, M.; Hill, M. S.; Kociok-Köhn, G. *Organometallics* **2009**, *28*, 1730.
(5) Datta, S.; Gamer, M. T.; Roesky, P. W. *Organometallics* **2008**, *27*, 1207.
(6) (a) Li, Y.; Marks, T. J. *Organometallics* **1996**, *15*, 3770. (b) Ryu, J.-S.; Li, Y.; Marks, T. J. *J. Am. Chem. Soc.* **2003**, *125*, 12584.

JA905615A